Electronics with Correlated Oxides: SrVO$_3$/SrTiO$_3$ as a Mott Transistor

Zhicheng Zhong,[1] Markus Wallerberger,[1] Jan M. Tomczak,[1] Ciro Taranto,[1] Nicolaus Parragh,[2]
Alessandro Toschi,[1] Giorgio Sangiovanni,[2] and Karsten Held[1]

[1]*Institute of Solid State Physics, Vienna University of Technology, A-1040 Vienna, Austria*
[2]*Universität Würzburg, Am Hubland, D-97074 Würzburg, Germany*

We employ density functional theory plus dynamical mean field theory and identify the physical origin of why two layers of SrVO$_3$ on a SrTiO$_3$ substrate are insulating: the thin film geometry lifts the orbital degeneracy, which in turn triggers a first-order Mott-Hubbard transition. Two layers of SrVO$_3$ are just at the verge of a Mott-Hubbard transition and hence ideally suited for technological applications of the Mott-Hubbard transition: the heterostructure is highly sensitive to strain, electric field, and temperature. A gate voltage can also switch between metal (ON) and insulator (OFF), so that a transistor with ideal ON-OFF switching properties is realized.

In the last years, there has been tremendous experimental progress to grow oxide heterostructures atomic layer by atomic layer, brought about by modern deposition techniques such as molecular beam epitaxy and pulsed laser deposition. A key experiment has been the discovery that a two-dimensional electron gas with high mobility is created at the interface of two band insulators, LaAlO$_3$ and SrTiO$_3$ [1]. This raised the hope that oxide heterostructures might substitute conventional semiconductor electronics one day, at least for specific applications [2,3]. Oxide electronics is however still in its infancy compared to the matured field of silicon electronics. Particularly promising are transistors at the scale of 2 nm [4], solar cells [5–7], and the possibility to generate spin-polarized currents [8]. Last but not least, there is high hope that strong electronic correlations make a difference to conventional semiconductors and give rise to new phenomena [9–11].

However, many oxide heterostructures, including the LaAlO$_3$/SrTiO$_3$ prototype, actually do not show strong electronic correlations. Since electronic correlations are weak, band structure calculations on the basis of density functional theory (DFT), e.g., within the local density approximation (LDA) [12], or even a tight binding modeling [13], are sufficient: such calculations well reproduce or predict experiment, e.g., angular resolved photoemission spectra [14–16]. A heterostructure where electronic correlations do play a decisive role is, on the other hand, SrVO$_3$ grown on a SrTiO$_3$ substrate. In the bulk, SrVO$_3$ is a correlated metal with a moderate renormalization $\sim$2 of the bandwidth [17–19] and a kink in the energy-momentum dispersion [20–22]. SrVO$_3$ has been widely employed [17,21,23–25] as a test bed material for LDA + dynamical mean field theory (DMFT) calculations [27–30]. Quite surprisingly, recent experiments [31] have found that two layers of SrVO$_3$ grown on a SrTiO$_3$ substrate are insulating, not metallic [32]. On the basis of the one-band Hubbard

model it has been argued [31] that the reduced bandwidth of the thin film is responsible for the Mott-insulating state.

In this Letter, we present realistic DFT + DMFT calculations and pinpoint the origin of the insulator to the crystal field splitting of the orbitals, caused by the reduced symmetry of the ultrathin film. The reduced bandwidth and the enhanced Coulomb interaction of the thin film do not play the key role. Our calculations demonstrate the high sensitivity of SrVO$_3$ films. A Mott-Hubbard metal-insulator transition can be triggered by small changes of temperature, (uniaxial) pressure, a capping layer, or an electric field. This makes SrVO$_3$ grown on SrTiO$_3$ most promising for applications as sensors or as a Mott transistor with a gate voltage controlling the Mott-Hubbard transition.

Method.—We perform DFT + DMFT calculations for two layers of SrVO$_3$ on a substrate given by four unit cells of SrTiO$_3$ and a sufficiently thick vacuum of 10 Å along the z direction. We fix the in-plane (xy plane) lattice constant to the calculated equilibrium bulk value of the substrate $a_{SrTiO_3} = 3.92$ Å, and optimize the internal coordinates by DFT. The DFT calculations are performed using the all-electron full potential augmented plane-wave method of the WIEN2K package [33] with the generalized gradient approximation potential [34] and a $10 \times 10 \times 1$ k-point grid.

The DFT states near the Fermi level, mainly of vanadium t_{2g} orbital characters, are well localized and exhibit strong correlations beyond DFT and DFT + U. To properly include these correlation effects, we first perform a Wannier projection onto maximally localized [35] t_{2g} orbitals, using the WIEN2WANNIER package [36]. We supplement this t_{2g} Hamiltonian constructed from DFT by the local Kanamori Coulomb interaction, given by the intraorbital interaction U, the interorbital (averaged) interaction U', and the Hund's exchange and pair-hopping J; for the Hamiltonian see Ref. [37]. The constrained LDA technique for the bulk yields $U' = 3.55$ eV [17,21] and for

the Hund's exchange a reasonable value for early transition metal oxides: $J = 0.75$ eV (cf. the Supplemental Material [38]); $U = U' + 2J$ by symmetry. For the DMFT calculations we use the W2DYNAMICS package [37], which implements a continuous-time quantum Monte Carlo algorithm in the hybridization expansion [52]. We employ the maximum entropy method [53] for the analytical continuation of the spectra to real frequencies. For checking the validity of our findings we perform, besides $d(t_{2g})$-only, also $d + p$ DFT + DMFT calculations for SVO bulk, freestanding SVO, and SVO on STO, which yield very similar results, see the Supplemental Material [38]. All DMFT calculations are at room temperature if not stated otherwise.

Results.—Figure 1 shows the DFT and DFT + DMFT spectrum for two layers of $SrVO_3$ on a $SrTiO_3$ substrate, as well as bulk $SrVO_3$ for comparison. Within DFT, the xy states are showing (almost) the same spectrum as for the bulk. These states have their orbital lobes within the xy plane and can be well modeled with a nearest neighbor hopping that is only in plane [13]. Hence, the confinement along the z axis has little effect. The yz states (and by symmetry the xz states) have a nearest neighbor hopping along the z axis, which is cut off by the vacuum and the insulating $SrTiO_3$ substrate [13]. As a consequence these states become more one dimensional (y axis hopping only) and the yz bandwidth is reduced. The yz bands are also pushed up in energy since breaking the cubic symmetry leads to a crystal field splitting $\Delta = 0.18$ eV between xy and yz (xz) states.

This lifting of the orbital degeneracy has dramatic consequences when electronic correlations are taken into account. Indeed, it is the physical origin of why thin $SrVO_3$ films are insulating. Figures 1(c) and 1(d) show the DFT + DMFT spectra; the DMFT self energies and comparative $d + p$ calculations are given in the Supplemental Material [38]. For the topmost (surface) layer, we see that electronic correlations further push the yz (and xz) states up in energy; they are essentially depopulated. That means, on the other hand, that the xy states are half filled. Because of this effective one-band situation and the relatively large intraorbital Coulomb interaction U, the xy states are
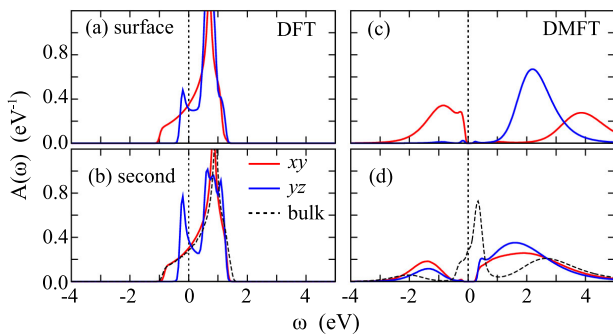
Mott-Hubbard split into an upper and lower Hubbard band. The $SrVO_3$ film is a Mott insulator. With the surface layer being insulating, also the second layer becomes a Mott insulator, albeit here the difference betweent the xy and yz population is much less pronounced. Note that due to the DMFT self-consistency also a more insulating second layer feeds back into an even more insulating surface layer.

This mutual influence can be inferred from Fig. 2(a), which shows that both layers get insulating at the same interaction strength. Here, $\overline{A(0)} \equiv \beta G(\tau = \beta/2)/\pi$ ($\beta = 1/T$ is the inverse temperature) is the spectral function around the Fermi level averaged over a frequency interval $\sim T$; it can be calculated directly from the continuous-time quantum Monte Carlo data without analytic continuation.

Clearly, the phase transition is of first order, as demonstrated by the hysteresis loop upon increasing or decreasing U'. We have checked that at a higher temperature (600 K), the hysteresis goes away, similarly as for the one-band Hubbard model [54]. Figure 2(a) also shows that, while the two-layer $SrVO_3$ film is insulating, it is just on the verge of an insulator-to-metal transition. As we will see below, this makes the $SrVO_3$ film ($SrVO_3/SrTiO_3$ heterostructure) sensitive to small changes of the environment such as changing temperature or pressure, or applying an electric field.

The orbital occupations $n_{i\alpha\sigma} = \langle c_{i\alpha\sigma}^\dagger c_{i\alpha\sigma} \rangle$ of the two layers i and orbitals α in Fig. 2(b) reflect what we have already qualitatively inferred from the spectra in Fig. 1: the surface layer becomes fully orbitally polarized, whereas the second layer shows only small differences in the orbital occupation. We did not observe any spin ordering in DMFT. Figure 2(c) shows how the normalized double occupation
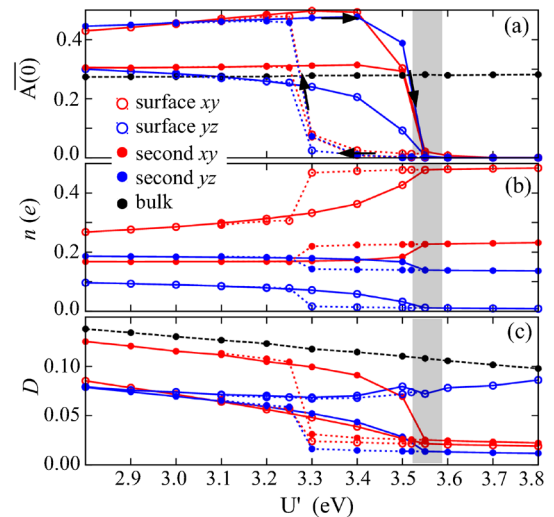
FIG. 2 (color online). Mott-Hubbard transition with increasing interaction U'; the gray shaded region indicates the estimated values of U' (see the Supplemental Material [38]). (a) Spectral function around the Fermi level $\bar{A}(\omega = 0)$—layer and orbitally resolved. (b) Orbital occupation. (c) Intraorbital double occupation. The solid (dotted) line is obtained when increasing (decreasing) U'.

FIG. 1 (color online). Layer-resolved spectral function of two $SrVO_3$ films grown on $SrTiO_3$ in DFT (a),(b) and DFT + DMFT at room temperature (c), (d). Dashed line: corresponding bulk spectrum.

$D_{i\alpha} = \langle c_{i\alpha\uparrow}^{\dagger} c_{i\alpha\uparrow} c_{i\alpha\downarrow}^{\dagger} c_{i\alpha\downarrow} \rangle / (n_{i\alpha\uparrow} n_{i\alpha\downarrow})$ drops at the Mott-Hubbard transition. The constant behavior of the surface layer yz orbital is simply due to the normalization (the numerator and denominator become extremely small).

Altogether, Figs. 1 and 2 show the typical behavior of a Mott-Hubbard transition in a multiorbital system that is controlled by the ratio of interaction to bandwidth and the orbital splitting. The latter is further enhanced by electronic correlations and is also crucial for $(Cr_xV_{1-x})_2O_3$ [55,56] as is the GdFeO$_3$ distortion for LaTiO$_3$ [23].

Physical origin of the Mott insulator.—By performing a number of additional calculations we have been able to identify the orbital symmetry breaking as the physical origin behind the dramatic difference between insulating SrVO$_3$ films and metallic SrVO$_3$ bulk. In Refs. [24,31] the reduction of the bandwidth due to cutting off the hopping perpendicular to the thin films (or surfaces) has been held responsible for the enhanced correlation effect and even the Mott-Hubbard transition. We calculated this effect: the reduction in bandwidth for the yz orbital is 20% and essentially zero for the xy orbitals. Following this picture, one would also expect an enhanced yz-orbital occupation [24], opposite to our findings.

Another possibility is an enhanced Coulomb interaction due to the reduced screening at the surface. To quantify this effect, we have performed constrained random phase approximation calculations (see the Supplemental Material [38]). This was (numerically) only possible for two freestanding SrVO$_3$ layers and yields ∼10% larger interactions. Such a calculation overestimates however the enhancement since the screening of the SrTiO$_3$ substrate is disregarded. A rough estimate is a 5% larger interaction strength than for the bulk.

Even when combining the reduced bandwidth and enhanced Coulomb interaction, this effect is by far insufficient to make SrVO$_3$ insulating: our DFT + DMFT calculations (not shown) still give a metallic phase for bulk SrVO$_3$ if the ratio of interaction to bandwidth is increased by 70%.

Instead, the key for the insulating nature of SrVO$_3$ films is the orbital symmetry breaking, given by the crystal field splitting and also the different bandwidths of the xy and yz (xz) orbitals. Electronic correlations largely amplify the small DFT orbital polarization, see Fig. 2. With the depopulation of the yz states, the surface SrVO$_3$ layer effectively becomes a one (xy) band system; and such a one-band system is a Mott insulator already at a much smaller interaction strength. Let us note that the lifting of the orbital symmetry was considered in Ref. [31] as a possible source for the observed deviations between theory and experiment and as a means to reduce the critical U'.

Surface shift of the lower Hubbard band.—Let us also emphasize the peculiar differences between the surface and second layer in Fig. 1. Besides the difference in occupation already discussed, also the position of the lower Hubbard band is shifted upwards by 0.5 eV in the surface layer; its weight and sharpness are enhanced. This effect might

actually explain the disagreement between photoemission spectroscopy (PES) and DFT + DMFT [17,57] regarding the position of the lower Hubbard band. As PES is surface sensitive, the surface layer will contribute strongly to the PES signal. In the Supplemental Material [38], we confirm that shift and sharpening are a general trend also observed for more (four) SrVO$_3$ layers; and we simulate PES spectra for different penetration depths. Including this surface effect leads to a better agreement with PES for bulk SrVO$_3$ (see the Supplemental Material [38]). A 20% upwards shift and a 10% narrowing of the lower Hubbard band in the surface layer has also been reported experimentally [58]. Let us note in passing that there is also a layer dependence of the quasiparticle weight in the metallic (more layer) case [10].

Sensitivity to external perturbations.—There has been a long quest to make use of strongly correlated electron systems and their huge responses upon small changes of the environment. As we have seen in Figs. 2(a) and 2(b), two insulating layers of SrVO$_3$ are at the edge of the hysteresis region. The (coexisting) metallic phase of SrVO$_3$/SrTiO$_3$ can still be stabilized if we slightly change the environment, e.g., (i) by pressure (which increases the bandwidth) or uniaxial strain (which controls the important splitting between the xy and yz orbitals), see Figs. 3(a) and 3(b), (ii) by decreasing the temperature to 200 K (see the Supplemental Material [38]), (iii) by one capping layer of SrTiO$_3$ on top of the SrVO$_3$ layers (see the Supplemental Material [38]), or (iv) by an external electric field of 0.01 V/Å, which corresponds to a voltage difference of 0.08 V across the two SrVO$_3$ layers, see Figs. 3(c) and 3(d).

Application as Mott transistor.—This electric field effect suggests that the SrVO$_3$/SrTiO$_3$ heterostructure is ideally suited for making a Mott transistor. In this respect, ON (metal) and OFF (insulator) are much better separated than in semiconductor transistors, where the change in conductivity with applied gate voltage is much more gradual than the first-order Mott-Hubbard transition. On the metallic side of the Mott-Hubbard transition, also a major part of all electrons contributes to the conductivity, not only a small number of doped charge carriers. Let us, in this context, also
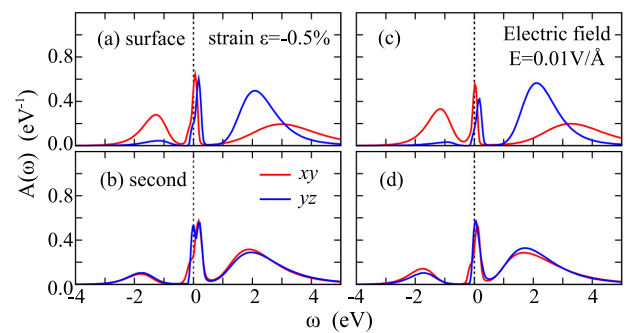

FIG. 3 (color online). A metallic solution, with a peak in the spectral functions $A(\omega)$ at the Fermi level ($\omega = 0$) in both SrVO$_3$ layers, can be stabilized with (a), (b) a compressive strain ϵ and (c), (d) an electric field E.

note the considerable experimental efforts to destabilize the (Mott or Peierls) insulating state of bulk VO_2 by an electric field using electrolyte gating [59,60], which might actually originate from field-induced oxygen vacancies [61,62].

The two layers of $SrVO_3$ on $SrTiO_3$ are just above the "upper" edge of the hysteresis region in Fig. 2. That is, the metallic solution is not stable any longer, but as we have seen in Fig. 3 it can still be stabilized by small perturbations. Switching from metal to insulator is hence no problem. The insulator is however quite stable: it requires a change in U' of ~ 0.2 eV (Fig. 2) or a change in Δ by ~ 0.15 eV (see the Supplemental Material [38]) before reaching the "lower" edge of the hysteresis loop in Fig. 2. This is difficult to achieve experimentally.

For a Mott transistor there is however another path to destabilize the insulator: doping it with only a very few electrons will turn the whole Mott insulator metallic, with a pronounced quasiparticle peak and a major part of the electrons contributing to the conductance, see Figs. 4(b) and 4(c). Such a doping might be achieved by adatoms or molecules on the $SrVO_3$ surface, and the system might hence act as a molecular sensor. For a transistor it is however preferable to have a protected surface, e.g., by an additional, insulating layer at the top. In this case applying a gate voltage will shift the t_{2g} states and eventually dope the Mott insulator, turning two insulating $SrVO_3$ layers metallic. In Fig. 4(a), we see that an effective gate voltage of 0.3 V is indeed sufficient to turn the two layers of $SrVO_3$ metallic. In our calculations we directly applied this effective gate voltage as a chemical potential shift eV_g. Due to geometry and distance, the actual gate voltage needed might be slightly higher. On the other hand, $SrTiO_3$ is a high-k dielectric, which reduces the actually needed gate voltage. Experiments have already demonstrated a similar amount of the doping as in Fig. 4(b) for other oxide heterostructures, see, e.g., Ref. [63] for $LaAlO_3/SrVO_3$. This confirms that realistic voltages allow us to switch the Mott transistor ON and OFF. Alternatively, an electron doping and hence metallicity might also be achieved by a nonequilibrium injection of charge carriers or a large source-drain voltage [64].
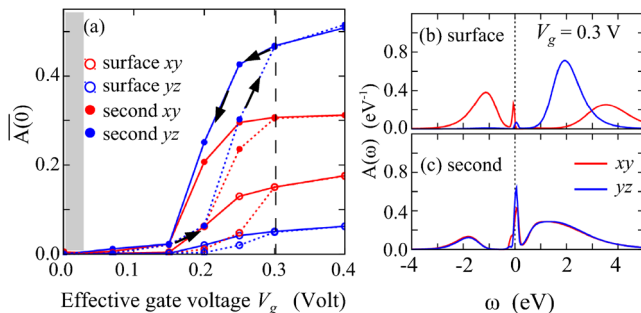
Let us note that also the application as a sensor is best combined with the above voltage effect. If we tune the voltage to the tipping point of the Mott transition, arbitrary small external perturbations will trigger the first-order transition. A quantitative measurement is possible by gauging what voltage is needed for reaching the Mott transition at a given temperature, pressure, number of adatoms, etc.

[1] A. Ohtomo and H. Y. Hwang, Nature (London) **427**, 423 (2004).

[2] J. Mannhart and D. G. Schlom, Science **327**, 1607 (2010).

[3] P. Zubko, S. Gariglio, M. Gabay, P. Ghosez, and J.-M. Triscone, Annu. Rev. Condens. Matter Phys. **2**, 141 (2011).

[4] C. Cen, S. Thiel, J. Mannhart, and J. Levy, Science **323**, 1026 (2009).

[5] E. Assmann, P. Blaha, R. Laskowski, K. Held, S. Okamoto, and G. Sangiovanni, Phys. Rev. Lett. **110**, 078701 (2013).

[6] H.-Z. Guo, L. Gu, Z.-Z. Yang, S.-F. Wang, G.-S. Fu, L. Wang, K.-J. Jin, H.-B. Lu, C. Wang, C. Ge, M. He, and G.-Z. Yang, Europhys. Lett. **103**, 47006 (2013).

[7] H. Liang, L. Cheng, X. Zhai, N. Pan, H. Guo, J. Zhao, H. Zhang, L. Li, X. Zhang, X. Wang *et al.*, Sci. Rep. **3**, 1975 (2013).

[8] N. Reyren, M. Bibes, E. Lesne, J.-M. George, C. Deranlot, S. Collin, A. Barthélémy, and H. Jaffrès, Phys. Rev. Lett. **108**, 186802 (2012).

[9] S. Okamoto and A. J. Millis, Nature (London) **428**, 630 (2004).

[10] S. Okamoto, Phys. Rev. B **84**, 201305(R) (2011).

[11] M. Jiang, G. G. Batrouni, and R. T. Scalettar, Phys. Rev. B **86**, 195117 (2012).

[12] R. O. Jones and O. Gunnarsson, Rev. Mod. Phys. **61**, 689 (1989).

[13] Z. Zhong, Q. Zhang, and K. Held, Phys. Rev. B **88**, 125401 (2013).

[14] K. Yoshimatsu, K. Horiba, H. Kumigashira, T. Yoshida, A. Fujimori, and M. Oshima, Science **333**, 319 (2011).

[15] A. F. Santander-Syro, O. Copie, T. Kondo, F. Fortuna, S. Pailhs, R. Weht, X. G. Qiu, F. Bertran, A. Nicolaou, A. Taleb-Ibrahimi *et al.*, Nature (London) **469**, 189 (2011).

[16] Z. Wang, Z. Zhong, X. Hao, S. Gerhold, B. Stoger, M. Schmid, J. Sanchez-Barriga, A. Varykhalov, C. Franchini, K. Held *et al.*, Proc. Natl. Acad. Sci. U.S.A. **111**, 3933 (2014).

[17] A. Sekiyama, H. Fujiwara, S. Imada, S. Suga, H. Eisaki, S. I. Uchida, K. Takegahara, H. Harima, Y. Saitoh, I. A. Nekrasov *et al.*, Phys. Rev. Lett. **93**, 156402 (2004).

[18] K. Maiti, U. Manju, S. Ray, P. Mahadevan, I. H. Inoue, C. Carbone, and D. D. Sarma, Phys. Rev. B **73**, 052508 (2006).

[19] M. Takizawa, M. Minohara, H. Kumigashira, D. Toyota, M. Oshima, H. Wadati, T. Yoshida, A. Fujimori, M. Lippmaa, M. Kawasaki *et al.*, Phys. Rev. B **80**, 235104 (2009).

FIG. 4 (color online).   (a) The hysteresis loop of the first-order Mott-Hubbard transition as a function of effective gate voltage V_g. (b),(c) At $V_g = 0.3$ V the spectral function $A(\omega)$ has developed a metallic peak; $V_g = 0.3$ V corresponds to 2% electron doping per V site or 2.5×10^{13} electrons/cm^2.

[20] K. Byczuk, M. Kollar, K. Held, Y.-F. Yang, I. A. Nekrasov, T. Pruschke, and D. Vollhardt, Nat. Phys. **3**, 168 (2007).

[21] I. A. Nekrasov, K. Held, G. Keller, D. E. Kondakov, T. Pruschke, M. Kollar, O. K. Andersen, V. I. Anisimov, and D. Vollhardt, Phys. Rev. B **73**, 155112 (2006).

[22] S. Aizaki, T. Yoshida, K. Yoshimatsu, M. Takizawa, M. Minohara, S. Ideta, A. Fujimori, K. Gupta, P. Mahadevan, K. Horiba *et al.*, Phys. Rev. Lett. **109**, 056401 (2012).

[23] E. Pavarini, S. Biermann, A. Poteryaev, A. I. Lichtenstein, A. Georges, and O. K. Andersen, Phys. Rev. Lett. **92**, 176403 (2004).

[24] A. Liebsch, Phys. Rev. Lett. **90**, 096401 (2003).

[25] As well as for GW + DMFT calculations, see Refs. [26,57].

[26] J. M. Tomczak, M. Casula, T. Miyake, F. Aryasetiawan, and S. Biermann, Europhys. Lett. **100**, 67001 (2012).

[27] G. Kotliar, S. Y. Savrasov, K. Haule, V. S. Oudovenko, O. Parcollet, and C. A. Marianetti, Rev. Mod. Phys. **78**, 865 (2006).

[28] K. Held, Adv. Phys. **56**, 829 (2007).

[29] For layer calculations with DMFT, see M. Potthoff and W. Nolting, Phys. Rev. B **60**, 7834 (1999); J. K. Freericks, *Transport in Multilayered Nanostructures: the Dynamical Mean-Field Theory Approach* (Imperial College Press, London, 2006); For nanoscopic calculations, see S. Florens, Phys. Rev. Lett. **99**, 046402 (2007); S. Biermann, A. Georges, A. Lichtenstein, and T. Giamarchi, Phys. Rev. Lett. **87**, 276405 (2001); M. Snoek, I. Titvinidze, C. Tőke, K. Byczuk, and W. Hofstetter, New J. Phys. **10**, 093008 (2008); A. Valli, G. Sangiovanni, O. Gunnarsson, A. Toschi, and K. Held, Phys. Rev. Lett. **104**, 246402 (2010).

[30] For DFT + DMFT calculations of a LaTiO$_3$/SrTiO$_3$ heterostructure [29], where a Mott and a band insulator get metallic at the interface, see F. Lechermann, L. Boehnke, and D. Grieger, Phys. Rev. B **87**, 241101(R) (2013).

[31] K. Yoshimatsu, T. Okabe, H. Kumigashira, S. Okamoto, S. Aizaki, A. Fujimori, and M. Oshima, Phys. Rev. Lett. **104**, 147601 (2010).

[32] Weakly correlated surfaces usually stay metallic to a single layer, see, e.g., R. Arita, Y. Tanida, S. Entani, M. Kiguchi, K. Saiki, and H. Aoki, Phys. Rev. B **69**, 235423 (2004).

[33] P. Blaha, K. Schwarz, G. K. H. Madsen, D. Kvasnicka, and J. Luitz, *WIEN2κ, An Augmented Plane Wave+Local Orbitals Program for Calculating Crystal Properties* (Karlheinz Schwarz, Techn. Universität Wien, Austria, 2001).

[34] J. P. Perdew, K. Burke, and M. Ernzerhof, Phys. Rev. Lett. **77**, 3865 (1996).

[35] A. A. Mostofi, J. R. Yates, Y.-S. Lee, I. Souza, D. Vanderbilt, and N. Marzari, Comput. Phys. Commun. **178**, 685 (2008).

[36] J. Kuneš, R. Arita, P. Wissgott, A. Toschi, H. Ikeda, and K. Held, Comput. Phys. Commun. **181**, 1888 (2010).

[37] N. Parragh, A. Toschi, K. Held, and G. Sangiovanni, Phys. Rev. B **86**, 155158 (2012).

[38] See Supplemental Material at http://link.aps.org/supplemental/10.1103/PhysRevLett.114.246401 for the cRPA calculation of the Coulomb interaction, the effect of T and a capping layer, as well as $d + p$ calculations, which includes Refs. [39–51].

[39] N. Parragh, Ph.D. Thesis, Universität Würzburg. 2013.

[40] N. Parragh, G. Sangiovanni, P. Hansmann, S. Hummel, K. Held, and A. Toschi, Phys. Rev. B **88**, 195116 (2013).

[41] F. Aryasetiawan, M. Imada, A. Georges, G. Kotliar, S. Biermann, and A. I. Lichtenstein, Phys. Rev. B **70**, 195104 (2004).

[42] N. Marzari and D. Vanderbilt, Phys. Rev. B **56**, 12847 (1997).

[43] T. Miyake and F. Aryasetiawan, Phys. Rev. B **77**, 085122 (2008).

[44] J. M. Tomczak, T. Miyake, R. Sakuma, and F. Aryasetiawan, Phys. Rev. B **79**, 235133 (2009).

[45] M. Casula, P. Werner, L. Vaugier, F. Aryasetiawan, T. Miyake, A. J. Millis, and S. Biermann, Phys. Rev. Lett. **109**, 126408 (2012).

[46] V. I. Anisimov, J. Zaanen, and O. K. Andersen, Phys. Rev. B **44**, 943 (1991).

[47] P. Hansmann, N. Parragh, A. Toschi, G. Sangiovanni, and K. Held, New J. Phys. **16**, 033009 (2014).

[48] K. Haule, C.-H. Yee, and K. Kim, Phys. Rev. B **81**, 195107 (2010).

[49] H. T. Dang, A. J. Millis, and C. A. Marianetti, Phys. Rev. B **89**, 161113 (2014).

[50] K. Morikawa, T. Mizokawa, K. Kobayashi, A. Fujimori, H. Eisaki, S. Uchida, F. Iga, and Y. Nishihara, Phys. Rev. B **52**, 13711 (1995).

[51] A. Amaricci, N. Parragh, M. Capone, and G. Sangiovanni, arXiv:1310.3043.

[52] E. Gull, A. J. Millis, A. I. Lichtenstein, A. N. Rubtsov, M. Troyer, and P. Werner, Rev. Mod. Phys. **83**, 349 (2011).

[53] M. Jarrell and J. Gubernatis, Phys. Rep. **269**, 133 (1996).

[54] A. Georges, G. Kotliar, W. Krauth, and M. Rozenberg, Rev. Mod. Phys. **68**, 13 (1996).

[55] G. Keller, K. Held, V. Eyert, D. Vollhardt, and V. I. Anisimov, Phys. Rev. B **70**, 205116 (2004).

[56] A. I. Poteryaev, J. M. Tomczak, S. Biermann, A. Georges, A. I. Lichtenstein, A. N. Rubtsov, T. Saha-Dasgupta, and O. K. Andersen, Phys. Rev. B **76**, 085127 (2007).

[57] C. Taranto, M. Kaltak, N. Parragh, G. Sangiovanni, G. Kresse, A. Toschi, and K. Held, Phys. Rev. B **88**, 165119 (2013).

[58] J. Laverock, B. Chen, K. E. Smith, R. P. Singh, G. Balakrishnan, M. Gu, J. W. Lu, S. A. Wolf, R. M. Qiao, W. Yang *et al.*, Phys. Rev. Lett. **111**, 047402 (2013).

[59] M. Nakano, K. Shibuya, D. Okuyama, T. Hatano, S. Ono, M. Kawasaki, Y. Iwasa, and Y. Tokura, Nature (London) **487**, 459 (2012).

[60] For thermochromic applications of VO$_2$, see J. M. Tomczak and S. Biermann, Phys. Status Solidi B **246**,1996 (2009).

[61] J. Jeong, N. Aetukuri, T. Graf, T. D. Schladt, M. G. Samant, and S. S. P. Parkin, Science **339**, 1402 (2013).

[62] Let us also note the switching between metal and insulator in manganites achieved by an electric field in A. Asamitsu, Y. Tomioka, H. Kuwahara, and Y. Tokura1, Nature (London) **388**, 50 (1997).

[63] A. D. Caviglia, S. Gariglio, N. Reyren, D. Jaccard, T. Schneider, M. Gabay, S. Thiel, G. Hammerl, J. Mannhart, and J.-M. Triscone, Nature (London) **456**, 624 (2008).

[64] V. Guiot, L. Cario, E. Janod, B. Corraze, V. Ta Phuoc, M. Rozenberg, P. Stoliar, T. Cren, and D. Roditchev, Nat. Commun. **4**, 1722 (2013); For nonequilibrium DMFT, see H. Aoki, N. Tsuji, M. Eckstein, M. Kollar, T. Oka, and P. Werner, Rev. Mod. Phys. **86**, 779 (2014).